Research Report

Performance Analysis of Magnetic Recording Systems

R. D. Cideciyan[1], E. Eleftheriou[1], and S. Tomasin[2]

[1]IBM Research
Zurich Research Laboratory
8803 Rüschlikon
Switzerland
{cid,ele}@zurich.ibm.com

[2]University of Padova
Via G. Gradenigo 6A
35131 Padova
Italy
tomasin@dei.unipd.it

Performance Analysis of Magnetic Recording Systems

R. D. Cideciyan and E. Eleftheriou

IBM Research, Zurich Research Laboratory, 8803 Rüschlikon, Switzerland

S. Tomasin

University of Padova, Via G. Gradenigo 6A, 35131 Padova, Italy, tomasin@dei.unipd.it

Abstract

Approximations to the union bound performance of sequence detection in the presence of colored noise and an algorithm to compute bit error and error event probabilities are presented and compared to bit-by-bit simulation results. These computations, which are very accurate at bit error probabilities $\leq 10^{-3}$, are then used to analyze the performance of standard and reverse concatenated Reed-Solomon(RS)/modulation coding schemes for generalized partial-response channels corrupted by colored noise. The analysis is used to determine the optimum RS code rate for recording systems that are of current interest.

1   Introduction

Partial-response class 4 (PR4) and extended PR4 channels (see [1] and references therein) have been the state of the art in disk drives until quite recently. At high linear densities, generalized partial-response polynomials with real coefficients provide a better match to the discrete-time response of the recording channel than monic polynomials with integer coefficients do. This class of polynomials, when combined with sequence detection, gives rise to noise-predictive maximum likelihood (NPML) systems [2], [3]. Currently, 16-state NPML detectors for generalized partial-response channels with a first-order null at DC operating at rates close to 1 Gbit/s represent the state of the art in the disk-drive industry.

Error control coding has played an important role in the design of recording systems. In disk drives the usual coding scheme for partial-response recording channels is concatenated coding with an outer Reed-Solomon (RS) code and an inner modulation/parity code [4]. In this type of coding scheme, known also as standard concatenation, the use of high-rate modulation codes with large block sizes leads to weak code constraints or an increase of error propagation at the modulation decoder. This fact, coupled with the desire to perform soft-decision decoding, has led to renewed interest in reverse concatenation [5]. For a PR4 sequence detector and a concatenated coding scheme based on RS codes with 8-bit symbols and rate-16/17 modulation codes, reverse concatenation permits the use of three interleaved RS codewords per sector, whereas standard concatenation requires at least four interleaved RS codewords per sector to achieve good overall performance [6].

Union bounds for intersymbol interference channels that estimate the performance of a sequence detector in the presence of white and colored Gaussian noise have been derived in [7] and [8], respectively. An exact computation of these union bounds using generating-function methods similar to those employed in [7] and [8] is possible only in the case of white Gaussian noise because the noise variance associated with an error event in the presence of colored noise depends on the particular error event under consideration. Here we present approximations to the union bound in [8] and an algorithm to compute bit error and error event probabilities for sequence detection in the presence of colored noise. These probabilities are used to evaluate the overall performance of a recording system by following an analytic approach similar to that given in [6].

In Section II, the recording system model is described and the equivalent discrete-time model of the recording channel is introduced in the form of a generalized partial-response channel impaired by colored noise. In Section III, methods of computing approximations to the bit error and error event probabilities at the output of a Viterbi detector are developed and compared to results obtained by computer simulation. In Section IV, the performance of standard and reverse concatenated RS/modulation coding schemes for generalized partial-response channels corrupted by colored noise is analyzed.

2   Recording System Model

A block diagram of the recording system model is shown in Fig. 1. The outer RS code operates on 8-bit symbols (bytes) and can correct up to t bytes per codeword. A 512-byte sector is encoded into $I = 3$ or 4 RS codewords that are byte-interleaved and fed to the modulation encoder. The inner code is a high-rate modulation code that imposes constraints to aid timing/gain recovery and avoid quasicatastrophic error propagation at the output of the sequence detector.

The binary outputs of the modulation encoder are mapped into bipolar symbols $+1$ and -1, written onto the disk in the form of a positive or negative magnetization along a circular track. The data
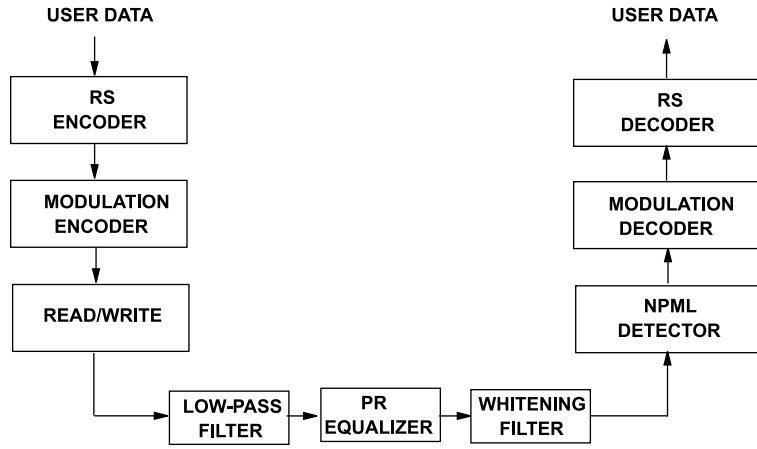
Figure 1: Recording system model.

sequence is read back from the head/disk assembly as an analog signal. After low-pass filtering and sampling, the signal is shaped into a partial-response signal format by the equalizer. The power of the total distortion at the output of the equalizer is reduced by noise prediction [2], [9]. Adopting a linear model for the read/write process, the chain of signal-processing functions including read/write heads, preamplifier, automatic gain control, low-pass filtering, sampling, equalization and noise whitening is modeled by the generalized partial-response polynomial $F(D) = 1 + \sum_{i=1}^{L} f_i D^i$, where L is the channel memory and f_i are real coefficients.

Figure 2 depicts the equivalent discrete-time model of the recording channel extending from the output of the modulation encoder to the input of the sequence detector. The input data sequence $\{x_k\}$ to the generalized partial-response channel is bipolar, i.e., $x_k \in \{-1, +1\}$. The sequence of colored noise samples $\{\eta_k\}$ at the input of the sequence detector is generated by passing the sequence of white noise samples $\{n_k\}$ through an equivalent filter $h(D)$ that represents the combination of the low-pass filter, the equalizer and the whitening filter. Finally, the sequence detector provides delayed estimates $\{\hat{x}_k\}$ of the bipolar symbols fed to the recording channel.
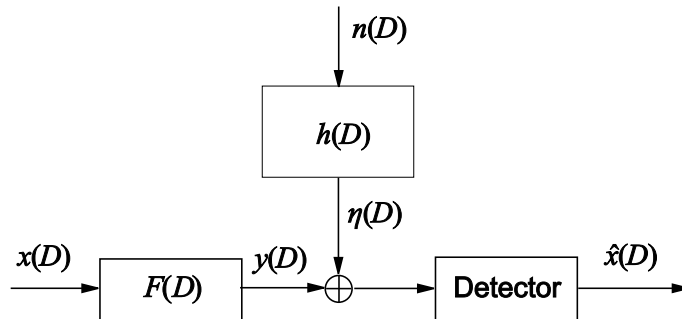

Figure 2: Equivalent discrete-time channel model.

3   Detector Performance in the Presence of Colored Noise

Let $\mathcal{E}$ be an error event of length i characterized by the input error sequence $\epsilon_x(D) = x(D) - \hat{x}(D)$ of length i. As the generalized partial-response channel is linear and time-invariant, the output error sequence can be expressed as $\epsilon_y(D) = \epsilon_x(D)F(D)$. The squared Euclidean distance associated with a particular error event $\mathcal{E}$ of length i is defined as the energy of the corresponding output error sequence of length $i + L$, i.e.,

$$d^2(\mathcal{E}) = ||\epsilon_y||^2. \tag{1}$$

At the output of a sequence detector, let E_i denote the set of all error events of length i, and b_i the probability that an error burst of length i starts at a particular time instant. The union bound states that the probability of a union of events is less than or equal to the sum of their individual probabilities. Hence,

$$b_i = \Pr(E_i) \le \sum_{\mathcal{E} \in E_i} \Pr(\mathcal{E}). \tag{2}$$

Similarly, an upper bound on the probability of bit error P_b at the output of the sequence detector is given by

$$P_b \le \sum_{\mathcal{E} \in E} w(\mathcal{E})\Pr(\mathcal{E}) \tag{3}$$

where $w(\mathcal{E})$ is the Hamming weight of the error event $\mathcal{E}$, which is defined as the number of nonzero coefficients in the corresponding input error sequence, $\Pr(\mathcal{E})$ is the probability of the error event $\mathcal{E}$, and E is the set of all possible error events.

In the following we classify the error events by their Euclidean distance. Let $\mathcal{E}^{(u,m)}$ be the m-th error event with distance d_u. Furthermore, $w_{u,m}$ denotes the Hamming weight of the error event $\mathcal{E}^{(u,m)}$, and $n(u, m)$ denotes the length of the corresponding output error sequence. Now we define the vector $V_{u,m}$ as the column vector corresponding to the normalized output error sequence, i.e.,

$$V_{u,m} = \frac{\epsilon_y\big(\mathcal{E}^{(u,m)}\big)}{||\epsilon_y(\mathcal{E}^{(u,m)})||}. \tag{4}$$

We now reformulate the bit error and error event probability results derived in [8] by using the error event classification introduced above. For this purpose the modified variance $\sigma_{u,m}^2$ associated with an error event $\mathcal{E}^{(u,m)}$ is defined as the variance along the vector $V_{u,m}$. The modified variance is given by the quadratic form

$$\sigma_{u,m}^2 = V_{u,m}^T \Phi V_{u,m}, \tag{5}$$

where Φ is the $n(u, m) \times n(u, m)$ covariance matrix associated with the sequence of colored noise samples $\{\eta_k\}$. The bit error probability of the sequence detector is then bounded by

$$P_b \le \sum_u \sum_m w_{u,m} Q\left(\frac{d_u}{2\sigma_{u,m}}\right) 2^{-w_{u,m}}, \tag{6}$$

where $Q(\cdot)$ represents the tail integral of the zero-mean, unit variance normal distribution, and $w_{u,m}$ denotes the Hamming weight of the m-th error event with distance d_u. Similarly, the error burst distribution b_i can be bounded by

$$b_i \le \sum_u \sum_m Q\left(\frac{d_u}{2\sigma_{u,m}}\right) 2^{-w_{u,m}}, \tag{7}$$

where now only error events $\mathcal{E}^{(u,m)} \in E_i$ that have distance d_u and length i are considered.

3.1 Approximations to the Union Bound

For maximum-likelihood sequence detection in the presence of white Gaussian noise it is common practice to obtain first-order approximations to union bounds by considering only error events with minimum distance. In the case of colored noise, the upper bounds on bit error and error event probabilities in Eqs. (6) and (7) are also obtained as a sum over infinitely many terms. However, the contribution of each term in Eqs. (6) and (7) is mainly determined by the ratio $\frac{d_u}{2\sigma_{u,m}}$ associated with an error event rather than just the Euclidean distance of an error event, as in the case of white noise. Consequently, the following approximations to the union bound consider only error events that satisfy the criterion

$$\frac{d_u}{2\sigma_{u,m}} \leq q_{\max},\qquad(8)$$

where q_{max} is a predetermined quantity that should be selected judiciously. We remark that, whereas the selection of error events according to their distance can be done efficiently in the white-noise case by exploring error flow graphs associated with the channel polynomial [7], [8], there is no simple solution for evaluating the modified variance. Therefore, to further simplify the selection of error events, an upper bound on the modified variance that depends on the length of the output error sequence is obtained. It can be shown that the following upper bound on the modified variance results from applying Schwarz's inequality to the quadratic form in (5)

$$\sigma_{u,m}^2 \leq \sigma^2 n(u,m)||h||^2,\qquad(9)$$

where σ^2 is the variance of the white noise $\{n_i\}$. The first sum in Eq. (6) can now be restricted only to error events that satisfy the condition

$$d_u \leq d_{\max} = 2q_{\max}\sigma\sqrt{n(u,m)}||h||,\qquad(10)$$

and the resulting approximate bound on the probability of bit error is

$$P_b \leq \sum_{u|d_u \leq d_{\max}} \sum_m w_{u,m} Q\left(\frac{d_u}{2\sigma_{u,m}}\right) 2^{-w_{u,m}}.\qquad(11)$$

Similarly, the burst error distribution b_i can be approximated as

$$b_i \leq \sum_{u|d_u \leq d_{\max}} \sum_m Q\left(\frac{d_u}{2\sigma_{u,m}}\right) 2^{-w_{u,m}},\qquad(12)$$

where again only error events $\mathcal{E}^{(u,m)}$ with distance d_u and length i are considered.

Summation over m in the above equations may involve an infinite number of terms with the same distance because of the presence of one or more zero-cycles [10]. A zero-cycle is a subevent $\epsilon_y(D)$ that can be repeated any number of times without accumulating Euclidean distance. There may be many zero-cycles in an error event. In general, the zero-cycles occur if the frequency response of the channel has spectral nulls. Magnetic recording channels have a spectral null at dc and therefore exhibit zero-cycles.

In the following we will call error events without zero-cycles elementary error events. Let us assume that n_{cyc} zero-cycles are inserted between elementary error events, i.e. the input error sequence is

$$\epsilon_x = \left[\epsilon_{x,1}\,\hat{\epsilon}_{x,1}\,\ldots\,\epsilon_{x,n_{\text{cyc}}}\,\hat{\epsilon}_{x,n_{\text{cyc}}}\,\epsilon_{x,n_{\text{cyc}}+1}\right],$$

where $\epsilon_{x,m}$ is an elementary subevent and $\hat{\epsilon}_{x,m}$ is a subevent made of the repetition of a zero-cycle.

As the filter $h(D)$ has finite length N_{eq}, $E[\eta_k \eta_i] = 0$, for $|k - i| > N_{\text{eq}}$, therefore $[\Phi]_{r,c} = 0$ for $|r - c| > N_{\text{eq}}$. Now, if the output error sequence is zero between the time instants k_1 and k_2 due to the presence of zero cycles, and $k_2 - k_1 > N_{\text{eq}}$, the modified variance of the noise can be expressed as

$$\sigma_{u,m}^2 = \sum_{r=1}^{k_1} \sum_{c=1}^{k_1} [V_{u,m}]_r [V_{u,m}]_c [\Phi]_{r,c} \tag{13}$$

$$+ \sum_{r=k_2}^{n(u,m)} \sum_{c=k_2}^{n(u,m)} [V_{u,m}]_r [V_{u,m}]_c [\Phi]_{r,c},$$

and this expression is independent of $|k_2 - k_1|$, the length of the zero-cycle. Therefore, if there is a sufficient number of zero-cycles, the argument of $Q(\cdot)$ in the above equations does not change.

Now let $\hat{w}_{u,m}$ denote the Hamming weight of a zero-cycle and $\sigma_{u,m}$ denote the modified variance of an elementary error event with Hamming weight $w_{u,m}$. Furthermore, we define $\hat{\chi}_{u,m} = 2^{-\hat{w}_{u,m}}$ and $\chi_{u,m} = 2^{-w_{u,m}}$. Finally, let $\mathcal{S}$ be the set of all two-tuples (u, m) such that (u, m) is associated with an elementary error event with Euclidean distance $d_u \leq d_{\text{max}}$. Then, the summation in (11) can be rewritten as follows

$$P_b \leq \sum_{(u,m) \in \mathcal{S}} Q\left(\frac{d_u}{2\sigma_{u,m}}\right) \left(\frac{w_{u,m} \chi_{u,m}}{1 - \hat{\chi}_{u,m}}\right.$$

$$\left. + \frac{\hat{w}_{u,m} \chi_{u,m} \hat{\chi}_{u,m}}{(1 - \hat{\chi}_{u,m})^2}\right). \tag{14}$$

Similarly, the burst error distribution can be expressed as

$$b_i \leq \sum_{(u,m) \in \mathcal{S}} Q\left(\frac{d_u}{2\sigma_{u,m}}\right) \left(\frac{\chi_{u,m}}{1 - \hat{\chi}_{u,m}}\right), \tag{15}$$

where the summation is over elementary error events with distance $d_u \leq d_{\text{max}}$ and length i.

3.2 A Search Algorithm for Evaluating Detector Performance

Here we give an algorithm that performs a modified depth-first search in an error flow graph. The search procedure identifies the error events that will be used to compute bit error and error event probabilities. Search algorithms for characterizing error events with specified distance at the output of partial-response channels of the form $(1 - D)^m (1 + D)^n$, $m, n \geq 0$ have been presented in [10].

The error flow graph is a directed graph that may be constructed as follows. The states are defined as the difference between the actual state of the generalized partial-response channel and the state estimated by the sequence detector. The edges connect nodes such that the first $L - 1$ elements of the initial state coincide with the last $L - 1$ elements of the terminal state. Each edge going from state $[\epsilon_x(k - 1), \epsilon_x(k - 2), \ldots, \epsilon_x(k - L)]$ to state $[\epsilon_x(k), \epsilon_x(k - 1), \ldots, \epsilon_x(k - L + 1)]$ is weighted with distance

$$\left(\epsilon_x(k) + \sum_{i=1}^{L} \epsilon_x(k - i) f_i\right)^2.$$

It is well known that the error flow graph is symmetric, i.e., the distance associated with an edge going from state $[\epsilon_x(k - 1), \epsilon_x(k - 2), \ldots, \epsilon_x(k - L)]$ to state $[\epsilon_x(k), \epsilon_x(k - 1), \ldots, \epsilon_x(k - L + 1)]$

is the same as that of the edge going from state $[-\epsilon_x(k-1), -\epsilon_x(k-2), \ldots, -\epsilon_x(k-L)]$ to state $[-\epsilon_x(k), -\epsilon_x(k-1), \ldots, -\epsilon_x(k-L+1)]$. This property of error flow graphs can be used to simplify the computations.

The algorithm starts from the zero state $[0, 0, \ldots, 0]$ and gradually extends the paths considering the successors of the zero state and then the successors of the successors and so on. Let us refer to the current path as the temporary path. The condition $\frac{d_u + d_{u,\text{end}}}{2\sigma_{u,m}} \leq q_{\max}$ is checked on each path extension, where $d_{u,\text{end}}$ is the minimum distance of the subpath going from the ending state of the temporary path to the zero state and $\sigma_{u,m}^2$ is the modified variance associated with the temporary path. The computation of $d_{u,\text{end}}$ is performed at the beginning of the algorithm, using a modified version of Dijkstra's algorithm [11]. Not all the temporary paths are considered and in particular the process of exploration of the successors stops when one of the following conditions is satisfied:

1. If the zero state is reached, the path is used for the computation of P_b from Eq. (14) and b_i from Eq. (15).

2. If the condition on the distance-to-modified variance ratio is not satisfied, the temporary path is discarded.

3. If the length of a zero-cycle repetition at the end of the temporary path exceeds N_{eq}, $\hat{w}$ and $\hat{\chi}$ are computed and no more cycles are allowed to grow at the end of the temporary path.
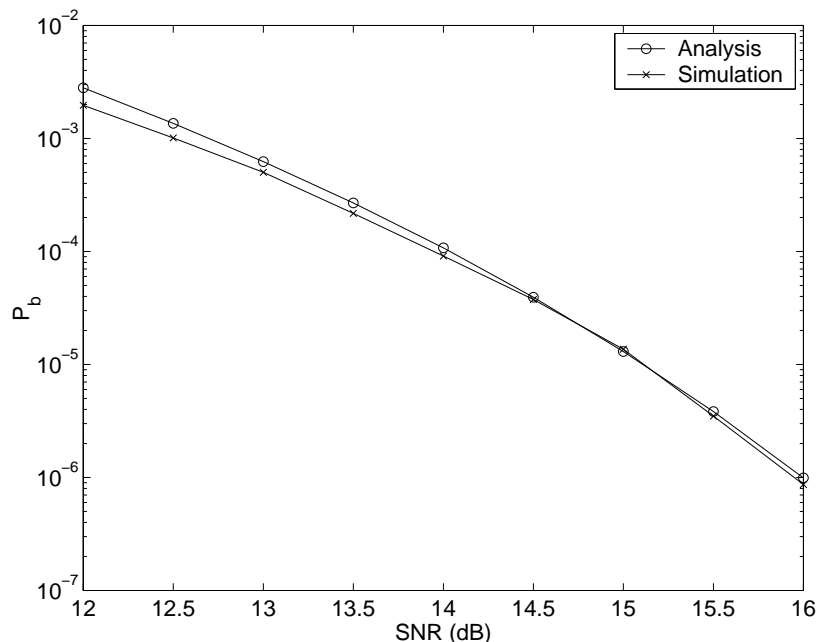
3.3   Simulation Results

Figure 3: Bit error probability as a function of SNR for $PW50/T = 2.5$.

The search algorithm presented above is used to compute the bit error probability at the output of a Viterbi detector for a degree-4 generalized partial-response channel corrupted by colored noise. The channel is characterized by the polynomial $F(D) = (1 - D^2)(1 + p_1 D + p_2 D^2)$, where the

target of the 10-coefficient equalizer has been assumed to be $(1 - D^2)$ and the predictor has two coefficients that have been optimized to minimize the noise power at the input of the detector. The read/write process extending from the output of the modulation encoder to the input of the lowpass filter has been modeled as a Lorentzian channel corrupted by additive white Gaussian noise. Thus, the noise at the 16-state detector input can be represented as filtered white noise where the filter corresponds to the combination of the lowpass filter, the 10-coefficient equalizer and the whitening filter $(1 + p_1 D + p_2 D^2)$ with two predictor coefficients.

Figure 3 shows the bit error probability as a function of the signal-to-noise ratio (SNR) for a Lorentzian channel with normalized linear density $PW50/T = 2.5$. The bit-by-bit simulation results agree well with the computed bit error probabilities. The results demonstrate that the computed approximations to the union bound are accurate for $P_b \leq 10^{-3}$. It is well known that union bounds are not tight at bit error probabilities $P_b > 10^{-3}$. Similarly, Fig. 4 shows the bit error probability as a function of the normalized linear density $PW50/T$ for SNR = 14 dB. Again we observe good agreement between the analytical results and bit-by-bit simulations.
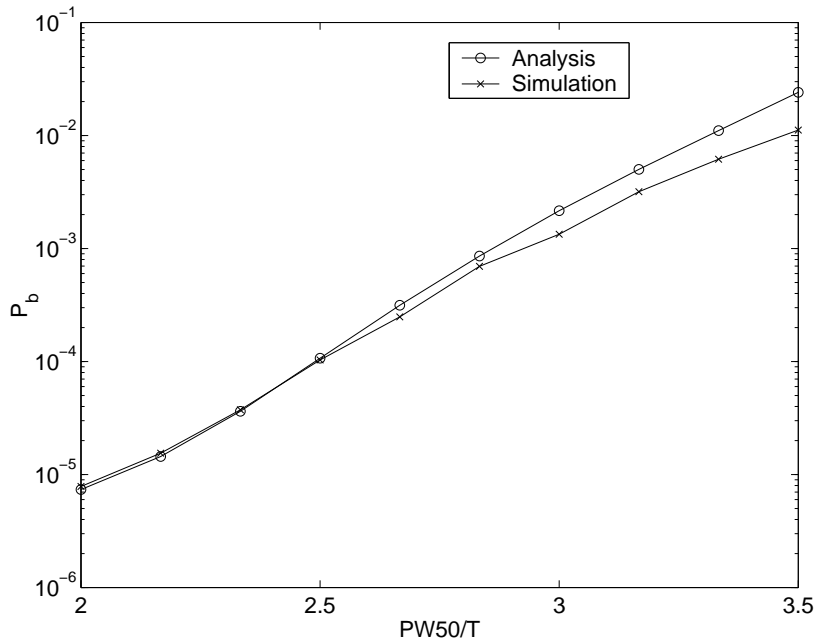

Figure 4: Bit error probability as a function of $PW50/T$ for SNR $= 14$ dB.

4 Recording System Performance

The performance of concatenated RS/modulation coding has been analyzed in [6] as a function of the code parameters and the polynomial

$$\tilde{b}(z) = \frac{1}{\sum_{i=1} b_i} \sum_{i=1} b_i z^i \tag{16}$$

that characterizes the burst error distribution at the input of the modulation decoder. This analysis applies to both standard and reverse concatenation and employs the sector error probability P_{sector} as

the performance measure. Furthermore, P_{sector} can be accurately estimated using the union bound IP_{decoder}, where P_{decoder} is the sum of the probability of decoder error and the probability of decoder failure.

The performance of concatenated RS/modulation coding (standard and reverse) for generalized partial-response channels will be analyzed based on the algorithm for computing the polynomial $\tilde{b}(z)$ discussed above. Specifically, we will compute the probability [6]

$$
P_{\text{decoder}} = \sum_{i=1}^{N_{\text{sector}}} \binom{N_{\text{sector}}}{i} b^i (1-b)^{N_{\text{sector}}-i} \left(\sum_{j=t+1}^{\infty} (q(z)^i)_j \right),
\tag{17}
$$

where $b = \sum_{i=1} b_i$, N_{sector} is the total number of recorded bits per sector and $q(z)$ is a polynomial that can be expressed as a function of $\tilde{b}(z)$. The subscript notation $(q(z)^i)_j$ indicates that the j-th coefficient of the polynomial $q(z)^i$ is used.

In the following we assume that the degree-4 generalized partial-response channel described in Section IIIC is used. Furthermore, a rate-16/17 modulation code is employed in standard concatenation where it is assumed that errors at the input of the modulation decoder cause two bytes to be in error. For reverse concatenation the same modulation code is used to encode user bytes, whereas a rate-8/9 modulation code is used to encode RS parity bytes. At a normalized user density $PW50/T_u = 2.6$, Fig. 5 compares the performance of standard and reverse concatenation schemes for $I = 3$ and 4 interleaves per sector, where each interleave can correct $t = 6$ bytes. After accounting for the rate increase due to RS and modulation coding, the normalized channel density $PW50/T$ is about 3. It can be seen that reverse concatenation permits the use of three interleaved RS codewords per sector, whereas standard concatenation requires at least four interleaved RS code-
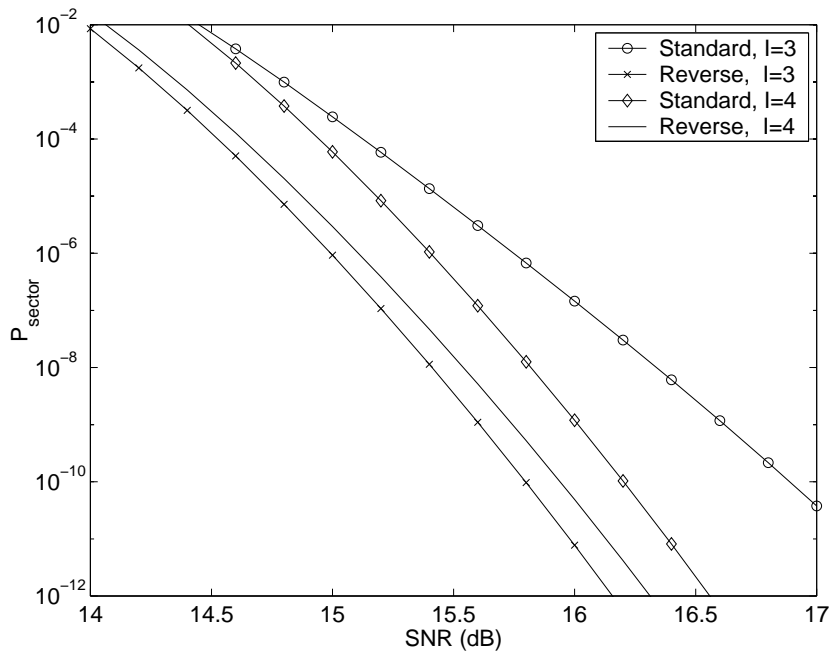

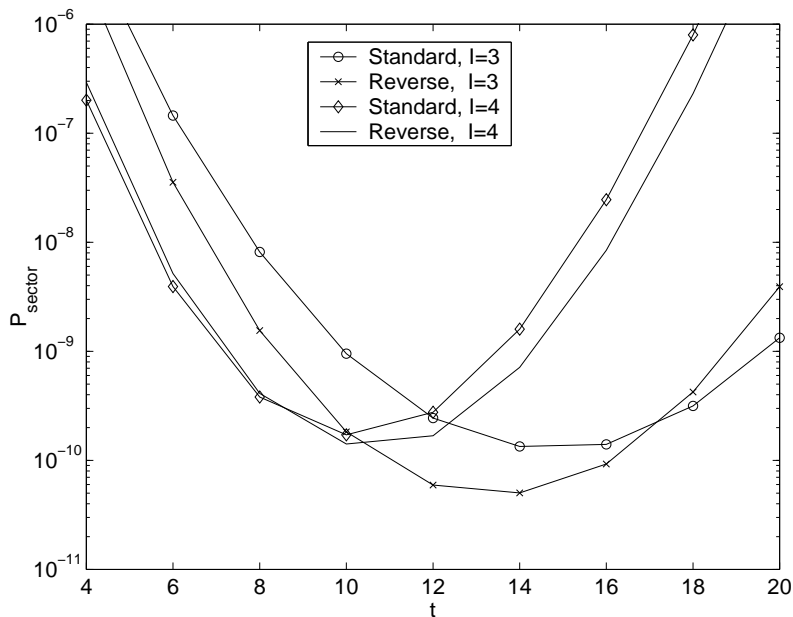Figure 5: Performance comparison for $t = 6$, $PW50/Tu = 2.6$.

Figure 6: Optimum RS code rate for $PW50/Tu = 2.6$.

words per sector to achieve good overall performance. Finally, Fig. 6 shows P_{sector} as a function of t for standard and reverse concatenation schemes with $I = 3$ and 4 interleaves per sector where $PW50/T_u = 2.6$ and SNR is fixed for each curve. The SNR values have been selected such that the minimum of P_{sector} is about 10^{-10}. It can be seen that in all four cases the optimum RS code rate is about 0.86.

5   Conclusions

The bit error and error event probabilities of Viterbi detectors for generalized partial-response channels that are corrupted by colored noise have been computed using approximations to union bounds and a modified depth-first search algorithm. The performance of standard and reverse concatenated RS/modulation coding schemes for generalized partial-response channels has been analyzed using the sector error probability as the performance measure. Computations have shown that the optimum RS code rate for current disk drive designs is about 0.86.

References

[1] R. D. Cideciyan, F. Dolivo, R. Hermann, W. Hirt, and W. Schott, "A PRML system for digital magnetic recording," *IEEE J. Select. Areas Commun.,* vol. 10, pp. 38-56, Jan. 1992.

[2] E. Eleftheriou and W. Hirt, "Noise-predictive maximum-likelihood (NPML) detection for the magnetic recording channel," *IEEE Conf. Records ICC'96,* pp. 556-560, June 1996.

[3] J. D. Coker, E. Eleftheriou, R. L. Galbraith, and W. Hirt, "Noise-predictive maximum-likelihood (NPML) detection," *IEEE Trans. Magn.,* vol. 34, pp. 110-117, Jan. 1998.

[4] R. D. Cideciyan, J. D. Coker, E. Eleftheriou, and R. L. Galbraith, "NPML detection combined with parity-based post-processing," *Digests of The Magnetic Recording Conf.,* Aug. 2000.

[5] W. G. Bliss, "Circuitry for performing error correction calculations on baseband encoded data to eliminate error propagation," *IBM Tech. Discl. Bull.,* pp. 4633-4634, Mar. 1981.

[6] J. L. Fan and A. R. Calderbank, "A modified concatenated coding scheme, with applications to magnetic data storage," *IEEE Trans. Inform. Theory,* vol. 44, pp. 1565-1574, July 1998.

[7] G. D. Forney, "Maximum-likelihood sequence estimation of digital sequences in the presence of intersymbol interference," *IEEE Trans. Inform. Theory,* vol. 18, pp. 363-378, May 1972.

[8] S. U. H. Qureshi and E. E. Newhall, "An adaptive receiver for data transmission over time-dispersive channels," *IEEE Trans. Inform. Theory,* vol. 19, pp. 448-457, July 1973.

[9] P. R. Chevillat, E. Eleftheriou, and D. Maiwald, "Noise predictive partial-response equalizers and applications," *IEEE Conf. Records ICC'92,* pp. 942-947, June 1992.

[10] S. A. Altekar, M. Berggren, B. E. Moision, P. H. Siegel, and J. K. Wolf, "Error-event characterization on partial-response channels," *IEEE Trans. Information Theory,* vol. 45, pp. 241-247, Jan. 1999.

[11] T. H. Cormen, C. E. Leiserson, and R. L. Rivest, *Introduction to Algorithms,* MIT Press, Cambridge MA, 1990.